Contents

1. Task **3**

2. Theoretical basics **4**

2.1. Spin 4
2.2. Magnetic moment 4
2.3. Magnetic resonance 4
2.4. Methods of measurement 6

3. Setup and procedure **8**

4. Data analysis **11**

4.1. Measurement of the magnetic field with the hall probe 11
4.2. Determination of the core magnetic moment of a ^{19}F-core 11
4.3. Determination of the gyro magnetic property of a proton in hydrogen 14
4.4. Determination of the gyro magnetic property of a proton in glycol 16
4.5. Fine measurement of the resonance frequency of a proton in hydrogen with the Lock-in-method 17

5. Summary and discussion **20**

A. List of Figures **22**

B. List of Tables **22**

C. References **22**

D. Appendix **24**

D.1. Additional Plots 24
D.2. Oscilloscope screenshots 26
D.3. Original data 27

1. Task

1. The magnetic field of the electromagnet shall be examined. Futhermore the homogenity of the field is to be analized.
2. The core-magnetic moment of the ^{19}F-core in teflon shall be determined.
3. The gyromagnetic proportion of the proton in hydrogen shall be determined.
4. The gyromagnetic proportion of the proton in glycol is to be determined.
5. The resonanz frequency of protons of the hydrogen probe shall be determined. For this the Lock-in-method is to be used.

2. Theoretical basics

Most of the equations and explanations in this chapter are based on [1]. If not they are labelled with their corresponding reference.

2.1. Spin

The inner angular momentum of a quantum mechanical particle is called spin. These particles can be separated in two groups: the fermions (with spin $s = \frac{1}{2}, \frac{3}{2}, ...$) and the bosons (integer spins). Electrons, protons and neutrons are fermions. The spin is quantized and takes, only specific absolute values

$$\left|\vec{S}\right| = \hbar\sqrt{S(S+1)}.$$

Here S is the spin quantum number with $S = 0, \frac{1}{2}, 1, ...$ Analogue to this there is a spin, the nuclear spin, in the core of an atom

$$\left|\vec{I}\right| = \hbar\sqrt{I(I+1)}.$$

I is the so called nuclear spin quantum number. If we take a fixed axis, the values we can get are

$$I_z = m_I \hbar,$$

with $m_I \in \{-I, -I+1, \ldots, 0, \ldots, I-1, I\}$. Therefore we can have $2I+1$ possible I_z.

2.2. Magnetic moment

Particles that have a spin, also must have a magnetic moment. These two are connected by the gyromagnetic relationship $\gamma = \frac{g_I \mu_k}{\hbar}$, with the constant core-g-factor g_I and the core magneton $\mu_k = \frac{e\hbar}{2m_p}$:

$$\vec{\mu} = \gamma \vec{I}.$$

According to the Pauli principle, every orbital can host two protons and two neutrons. The two protons must then have opposing spins. The same is the case for the neutrons. Following from this, it is obvious, that a core in its ground state, with an even number of protons and neutrons has a spin of $I = 0$, whereas one with an uneven number of one of the nucleon types, has a spin of $I = 1/2$.

2.3. Magnetic resonance

In an external magnetic field $\vec{B}$, a core with the magnetic moment $\vec{\mu}$ has the potential energy

$$E = -\vec{\mu} \cdot \vec{B}.$$

If we look at a field that is in a specific direction, for example in the z-direction, we get different energy levels with the magnetic quantum number m_I

$$E = -g_I \mu_K m_I B.$$

This is called the Zeeman effect. If we take a look at the energies of two energetical neighbours, meaning $\Delta m_I = \pm 1$, we get

$$\Delta E = g_I \mu_k B.$$

This energy ΔE is the amount of energy it takes to flip a spin of a particle into a higher energy level or the energy which gets emitted if the spin flips down again.
Besides interaction with other atom cores, there are spontaneous and or induced absorption and emission of photons to achieve excitement. Basically we can use the interaction with a radiation field (e.g. electro-magnetic). With this known energy ΔE needed, we can calculate the so called resonance frequency of the radiation field with

$$\nu = \frac{\Delta E}{h} = \frac{g_I \mu_k B}{h} = \frac{\gamma B}{2\pi}.$$

When resonating, the radiation field will loose or gain energy.
At thermal equilibrium, the population density on one energy level is Boltzmann distributed. Therefore the ratio of the population densities n of two energy levels ($E_{\text{high}} > E_{\text{low}}$) is

$$\frac{n_{\text{high}}}{n_{\text{low}}} = e^{-\frac{E_{\text{high}} - E_{\text{low}}}{kT}} = e^{-\frac{\Delta E}{kT}}.$$

Therefore the radiation field looses more energy than it gains. With that we would expect the ratio to level over time ($n_{\text{ratio}} = 1$), meaning the effect of the resonance would wear of, but in reality it does not. That's due to relaxation effects.

Spin-Lattice interaction [6]

Atoms that are bond in a molecular structure constantly vibrate, because of the heat of the system. The vibration of the charged particles in the atoms causes a complex magnetic field (see Maxwell equations). This field is called the lattice field. The lattice field interacts with both low and high energy state cores, which results in the higher energy states giving energy to the lower ones. Therefore a part of the energy gained from a spin flipping into a higher energy state gets dissipated into the lattice field, which results in a slightly faster vibration and therefore temperature. This energy is lost for the radiation field, because the photons, who get emitted, when the spin falls back down again, have a smaller energy than when they were absorbed.

Spin-Spin interaction

The other form of relaxation is called spin-spin interaction. The spin from one core produces a magnetic field at the location of a second atom core. This magnetic field can increase or decrease the applied magnetic field, and therefore the core has a slightly different resonance frequency.

Chemical shift

The third significant effect is the chemical shift. In a molecular structure, the atoms enter into chemical bonds with other atoms. In reality in each material we use are impurities, like foreign atoms. Those have a different resonance frequency. The bond with such atoms defines the shielding coefficient σ. The effective magnetic field which interacts with the cores is dependent on that coefficient

$$B_{eff} = (1-\sigma)B_0 \text{ [4]}.$$

Therefore the shielding coefficient changes the effective magnetic field and therefore changes the value of the resonance frequency.

2.4. Methods of measurement

Hall effect & hall probe

Charged particles in a magnetic field are influenced by said field. The equation, which describes the force that takes effect on the particles is the Lorentz force

$$\vec{F}_L = q\left(\vec{v}\times\vec{B}\right).^{\dagger} \tag{2.1}$$

If we observe a (block shaped) conductor, with a current and an external magnetic field applied, the electrons in the conductor move to one side according to equation 2.1. Therefore on one side of the conductor, there are more electrons than on the other side, meaning an electrical field is produced, with the force $F_E = qE^{\dagger\dagger}$. This force of the electric field starts to compensate the effect of the Lorentz force till they compensate each other and come to an equilibrium. Now we can derive the equation for the hall voltage:

$$\begin{aligned}
|\vec{F_E}| &= |\vec{F_L}| \\
q\cdot E &= q\cdot vB \\
\frac{U_H}{d} &= vB \\
U_H &= vBd.
\end{aligned}$$

We can see, that with a hall probe we can measure the magnetic field strength, if we apply a known voltage to a conductor. Taking the current into account, with $I = nevBd$ we get

$$U_H = \frac{I}{ne}. \tag{2.2}$$

By looking at eq. 2.2 we can derive, that a hall probe should be made out of semi-conducting material, because the lower the number n of electrons is, the higher the voltage gets.

Lock-in method

The lock-in method is used to optimise signals with a very bad signal to noise ratio. It makes signals visible again, even if the noise it 100 000 times larger than the signal.

To do so, we need a reference signal ($U_{\text{ref}} = U_0 \sin\omega t$), which has to have the same phase relation as our signal. Our magnetic field modulation signal is a saw tooth function with a sinus on top of it ($U(t) = U_{sz} + U_0 \sin\omega t$ shown in Figure 1). This signal influences the NMR signal and gives us our absorption signal. This signal gets multiplied by the reference signal and integrated, therefore filtering out all the signal with different phase relations than our reference signal.

To understand the filtering process, we need to look at the Taylor series expansion of our absorption signal:

$$A(U(t)) \approx A(U_{sz}) + \frac{dA}{dU} U_0 \sin\omega t. \tag{2.3}$$

When we multiply that with our reference signal and then integrate it, in the second part of (2.3) all the signals with a different phase relation vanish, because of the orthogonality relations of trigonometric functions

$$\int\limits_{-\infty}^{+\infty} \sin(\omega_1 x)\sin(\omega_2 x)dx = \delta(\omega_2 - \omega_1).$$

[†] The general equation also has a electric field in it: $\vec{F}_L = q\left(\vec{E} + \vec{v}\times\vec{B}\right)$.

[††] $E = \frac{U}{d}$, with d as the length of the conductor

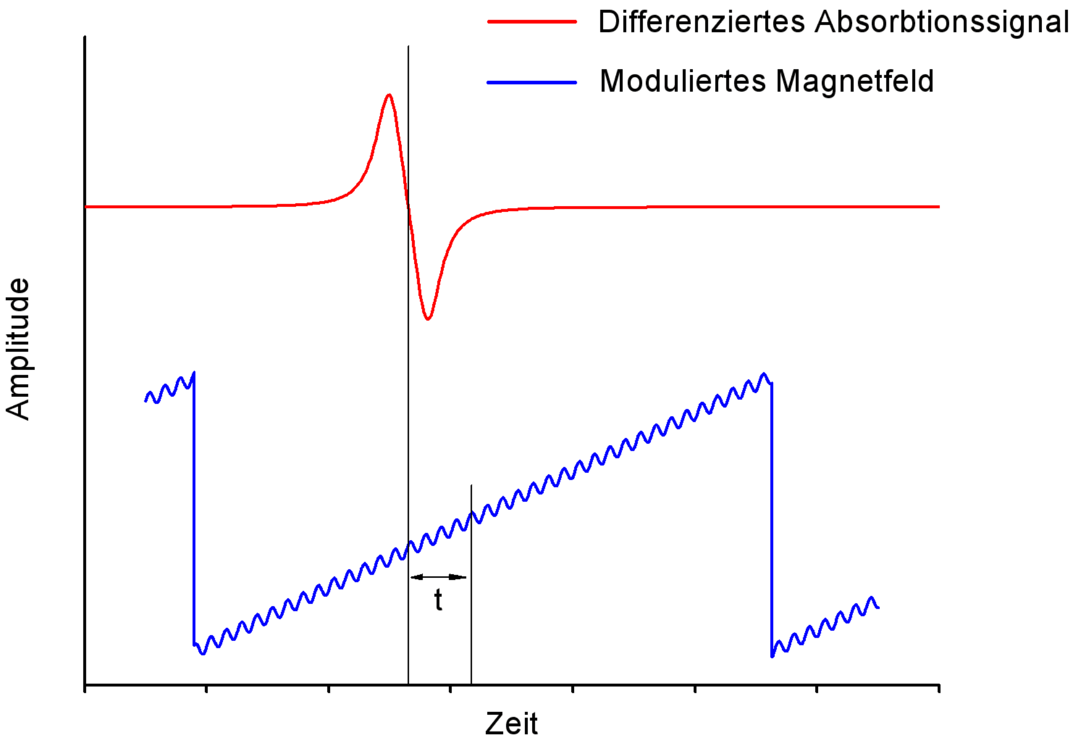

Figure 1: Differentiated absorption signal [1].

3. Setup and procedure

Setup

The setup for the measurement of the magnetic field is shown in figure 2.

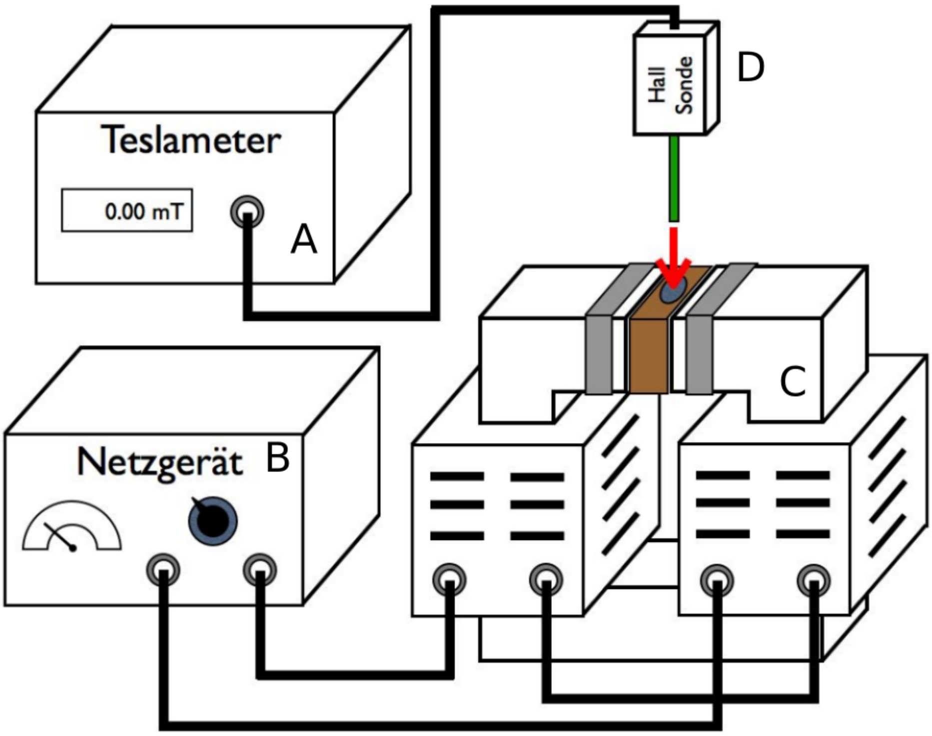

Figure 2: Setup for the measurement of the magnetic field [1].

It consists of a power supply (B) unit which is connected to an electromagnet (C). Between the magnet there is a hole in which we put a hall probe (D) which passes the measured data through to a teslameter (A). The depth to which the probe enters the magnetic field is measured with a measurement tape that is fixed to the probe. In order to get results, a fixed voltage and current have to be chosen on the power supply unit. Then the depth of the probe is varied. This has to be logged together with the amplitudes of the magnetic field.

The measurement apparatus for the testing of a ^{19}F-core-, a hydrogen- and a glycol-sample can be seen in figure 3.

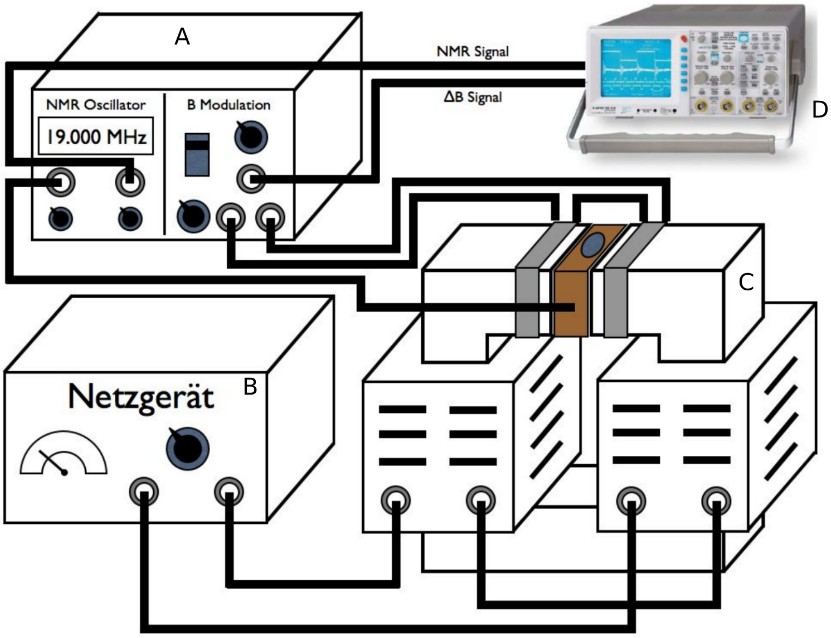

Figure 3: Setup for the measurements in exercise 2, 3 and 4 [1].

Again it has a power supply unit (B) and the electromagnet (C). But now there are also two electromagnets at the facing ends of the electromagnet, at which sinus modulated voltage is applied. Furthermore a HF-oscillator (A) is connected to the area between the electromagnet. The samples are inserted in the same hole as the hall probe before. The frequency generator is connected to an oscilloscope (D) that records the modulated electromagnetic field and the HF-signal that interacts with the sample. In this part the hall probe is only needed once before every measurement in order to know what the strength of the applied magnetic field is.

In the last part a hydrogen-sample gets measured with the Lock-in method. The setup is shown in figure 4.

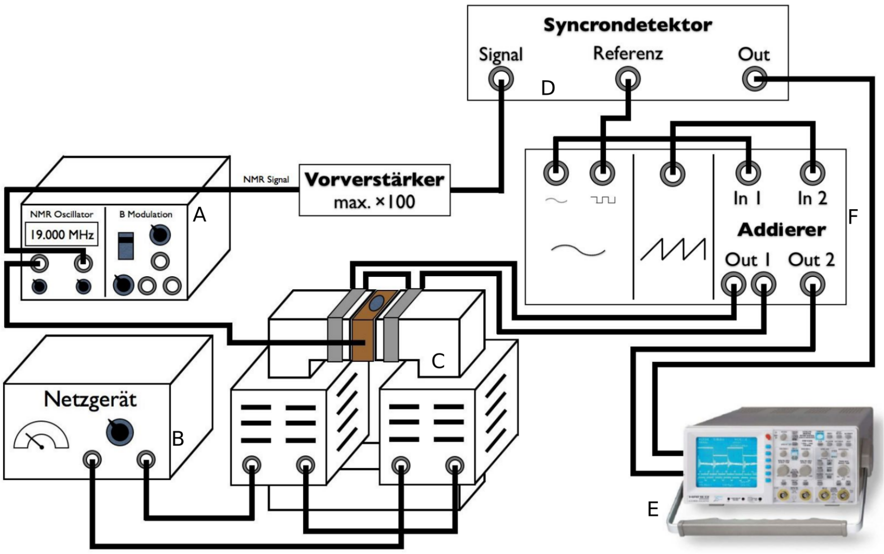

Figure 4: Setup for the measurement in exercise 5 [1].

It consists, as the setups before, of a power supply unit (B) and an electromagnet (C). There is also again an oscillator (A). But this time we also need an adder (F), in order to get a saw tooth signal on top of which there is a sine signal. The resulting signal gets from the interaction of the magnetic field with the sample, after it has been cleaned by the lock-in-method, can be looked at with an oscilloscope (E).

Procedure

We started by measuring our magnetic field, or more precise, we measured for its homogeneity. We did this by using the hall probe, sticking it in the magnet deeper and deeper. Each time we measured how deep it is and the value of the magnetic field strength. By looking at the data, we choose a point of depth at which we expect the field to be the most homogeneously and used it for the following measurements ($d = 2.0\,\mathrm{cm}$).

For the next three parts we needed the highly oscillating radiation field. We build the setup as shown in figure 3. As probes we used ^{19}F, ^{1}H and glycol. With the help of the given resonance frequencies for each probe we estimated the strength of the magnetic field needed to set our HF-frequency below 20 MHz, because the used frequency generator isn't capable of delivering a higher frequency. With the set magnetic field we started varying the frequency until we saw the resonance peaks. We then set them to be equidistant. Having achieved that, we exported the data from the oscilloscope as .csv and .png files. Then we zoomed in on one peak for the error measurement. For that we need four data sets. The first one is the frequency at which resonance starts. While rotating the frequency knob clockwise to increase its value, the shown frequency dropped at some point and started rising again after that. The second data set has to be just right before the drop happens and the third right after it. The fourth data set is at the last point where one can see some kind of resonance. With those four data sets we can calculate the error on the frequency (this is explained in the data analysis chapter).

In the last part we used the setup pictured in figure 4. The key difference is, that we now use a lock-in amplifier to get cleaner signals and hope to gain an overall more accurate measurement. After adjusting all the settings with a little help from our tutor[†], we saw the rising staircase function, which modulates our magnetic field, and the frequency with the resonance peak on the oscilloscope. We then changed the frequency to move the peak in the range of one full period of the modulation. We measured at eight different frequencies and exported the data as .csv files.

[†] He did everything. Thanks Stephen.

4. Data analysis

4.1. Measurement of the magnetic field with the hall probe

All our analysis was made with python. Because we wanted to get the graphs clearer we mostly didn't draw in errors and often connected the measured points with lines.
For the first measurement we chose a voltage of $U = (9.00 \pm 0.05)\,\mathrm{V}$ and a current of $A = (4.080 \pm 0.005)\,\mathrm{A}$.
In order to know whether the magnetic field is homogeneous or not we collected the data shown in figure 5. The corresponding data is in table 1. The read off error on the magnetic field is $s_B = 0.5\,\mathrm{mT}$ and that of the depth $s_d = 0.1\,\mathrm{cm}$.

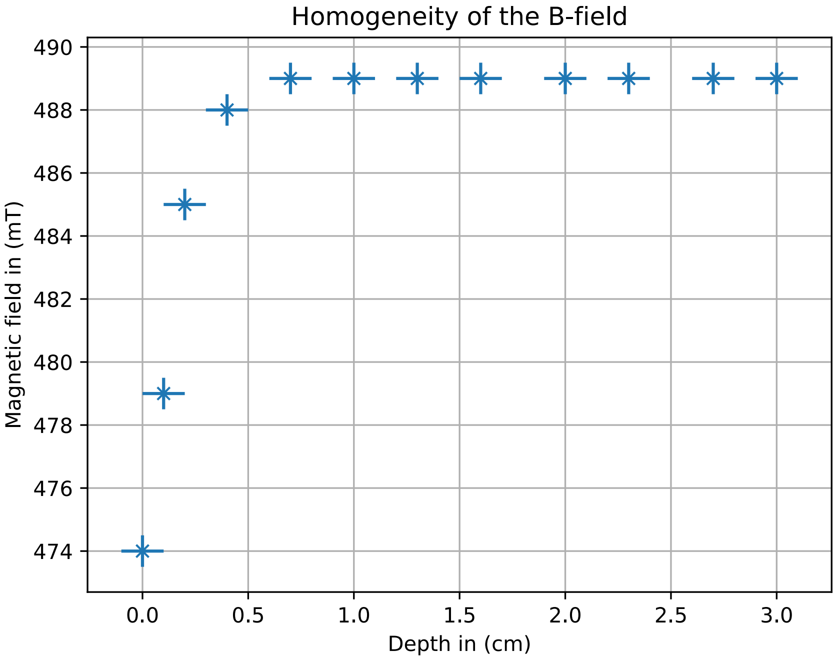

Figure 5: The value of the measured magnetic field plotted against the depth of the hall probe.

height [cm]	0	0.1	0.2	0.4	0.7	1	1.3	1.6	2	2.3	2.7	3
B-field [mT]	474	479	485	488	489	489	489	489	489	489	489	489

Table 1: Data of the measurement of the magnetic field with $s_B = 0.5\,\mathrm{mT}$ and $s_d = 0.1\,\mathrm{cm}$.

It can be seen, that below a depth of 0.7 cm the field is very homogeneous. The total error on the magnetic field in this part is still 0.5 mT, because we didn't measure any differences from the value $B = 489\,\mathrm{mT}$ and therefore didn't get a standard deviation from the mean value. The lower end we couldn't measure because the tape measure on the hall probe could not be read of at that depth. Because we had to re-adjust the current for each measurement we remeasured the magnetic field after each of them.

4.2. Determination of the core magnetic moment of a ^{19}F-core

The amplitude and the time distribution for a frequency of $\nu = (19.2396 \pm 0.0002)\,\mathrm{MHz}$ is shown in figure 6. This frequency was chosen, because there the peaks of the HF-signal had the same distance and the ways through zero were at the same points as those of the modulation signal.

This modulation signal is shrunk by a factor of fifty in order to fit into the diagram. A screen shot of the oscillator can be found in the appendix (fig. 29). We chose a B-field of $(480.0 \pm 0.5)\,\mathrm{mT}$. In the following we will take a closer look at the peak around $0\,\mathrm{s}$.

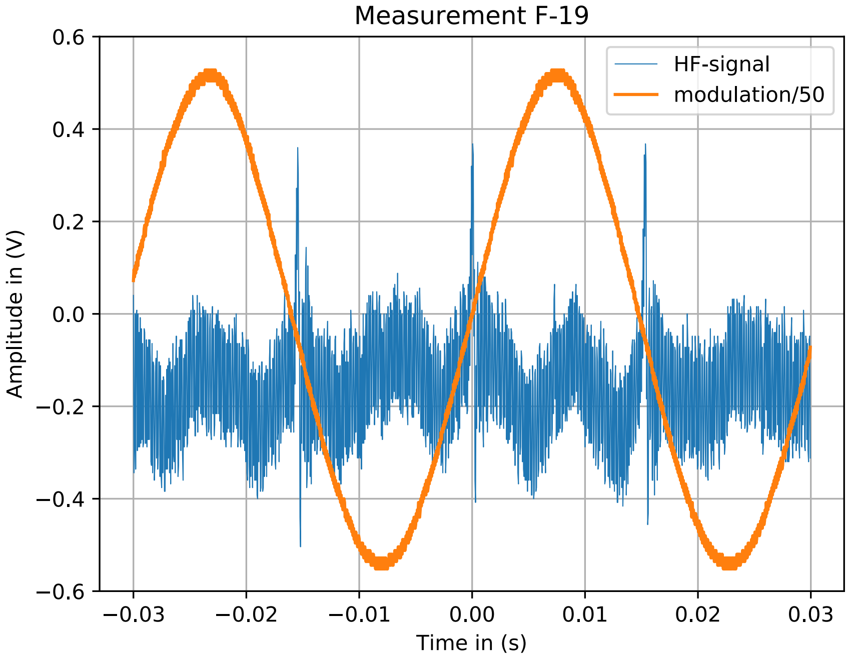

Figure 6: Data for ^{19}F with the modulation signal that is shrunk by a factor of 50.

The aim for the chosen frequency is, that the peaks of the signal (see fig 6) are equidistant. In order to get the error on the frequency we measured four times around the peak in the middle for slightly different frequencies. The first and the last measurement (blue and red curve in 7) got taken at frequencies for which there is no signal, but just noise, at $t \approx 0\,\mathrm{s}$. Turning the frequency dial, starting from the frequency of the blue curve, higher towards the frequency of the red curve, it can be seen, that at one point the frequency drops. This is a result of the setup. Physically we would expect the frequency to constantly rise, if we turn the dial of the frequency generator clockwise. In reality we observe the drop, because the generator is coupled to our system. Since we can't compensate this calibration off set, we do the described four measurements to calculate an error. The data of the orange and green plots were measured shortly before and after this drop. These plots are shown in figure 7. The reason, why we don't get sharp signals, but ones that oscillate back to zero, is because of the rule of Lenz. It says, that if a magnetic flux gets changed, then a capacity gets induced, which opposes the change of the magnetic field.

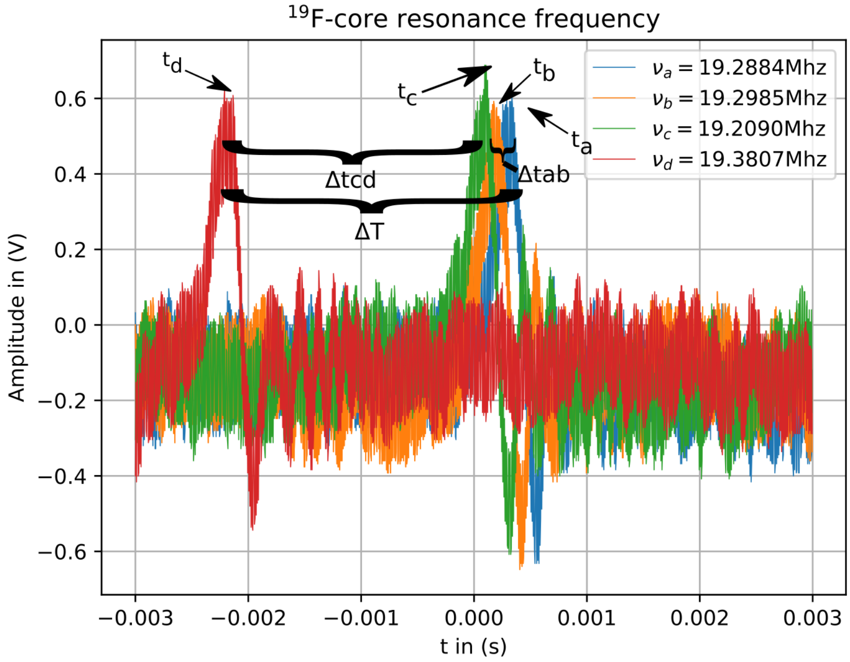

Figure 7: Method to determine the error of ν for ^{19}F.

From this plot then the error can be calculated with the formula:

$$s_\nu = \sqrt{\left(\frac{\Delta t_{ab}}{\Delta T}\cdot\Delta\nu_{ab}\right)^2 + \left(\frac{\Delta t_{cd}}{\Delta T}\cdot\Delta\nu_{cd}\right)^2}, \tag{4.1}$$

where Δt_{ab} and Δt_{cd} are the time differences between the peaks, ΔT is their sum and $\Delta\nu_{ab}$ and $\Delta\nu_{cd}$ are the differences between the frequencies we chose. For the values of the four peaks ($t_a = 0.000\,335\,\mathrm{s}$, $t_b = 0.000\,175\,\mathrm{s}$, $t_c = 9.5\cdot10^{-5}\,\mathrm{s}$, $t_d = -0.002\,210\,\mathrm{s}$) we get $s_\nu =$0.06 MHz. This gets added quadratic to the read-off error for the frequency which is $s_{\nu mess} = 0.0002\,\mathrm{MHz}$

$$s = \sqrt{s_\nu^2 + s_{\nu mess}^2},$$

although the read-off error also could be neglected. From this follows a frequency of

$$\boxed{\nu = (19.24 \pm 0.06)\,\mathrm{MHz}.}$$

The following formula from [1] allows us to calculate the gyro magnetic factor. Since we assume the core magneton and Planck's constant to be precise, with the formulas

$$g_I = \frac{\nu\cdot h}{\mu_K\cdot B}, \tag{4.2}$$

and

$$s_{g_I} = g_I\cdot\sqrt{\left(\frac{s_\nu}{\nu}\right)^2 + \left(\frac{s_B}{B}\right)^2},$$

and for $\mu_K = 3.152\,451\,255\,0\cdot10^{-8}\,\frac{\mathrm{eV}}{\mathrm{T}}$ from [2] we get

$$\boxed{g_I = 5.261 \pm 0.020.}$$

From this it is easy to get the gyro magnetic property

$$\gamma = \frac{g_I \cdot \mu_K}{h}, \tag{4.3}$$

with the value

$$\boxed{\gamma = (2.520 \pm 0.009) \cdot 10^8 \, \frac{\mathrm{rad}}{\mathrm{s\,T}},}$$

where the error is calculated as

$$s_\gamma = \gamma \cdot \left(\frac{s_{g_I}}{g_I} \right).$$

With this we then calculated the modulus of the magnetic moment. Since ^{19}F has a spin of $I = 1/2$, for the absolute value of the spin we get

$$|\vec{I}| = \hbar \sqrt{I(I+1)} = 5.7003 \cdot 10^{-16} \, \mathrm{eV\,s}.$$

The magnetic moment gets calculated with

$$\vec{\mu} = \gamma \vec{I},$$

and the error with

$$s_{|\vec{\mu}|} = |\vec{\mu}| \cdot \frac{s_\gamma}{\gamma}.$$

As the absolute value for the magnetic moment we get

$$\boxed{|\vec{\mu}| = (2.286 \pm 0.009) \cdot 10^{-8} \, \frac{\mathrm{eV}}{\mathrm{T}}.}$$

4.3. Determination of the gyro magnetic property of a proton in hydrogen

In this chapter and the following one we are going to use the same method as in the previous one. The only difference is that we will stop calculating once we know the gyro magnetic property and won't continue until we have calculated the magnetic moment.

This time the magnetic field is $B = (451.0 \pm 0.5)\,\mathrm{mT}$. The measured plot can be seen in figure 8, or in the appendix (figure 30).

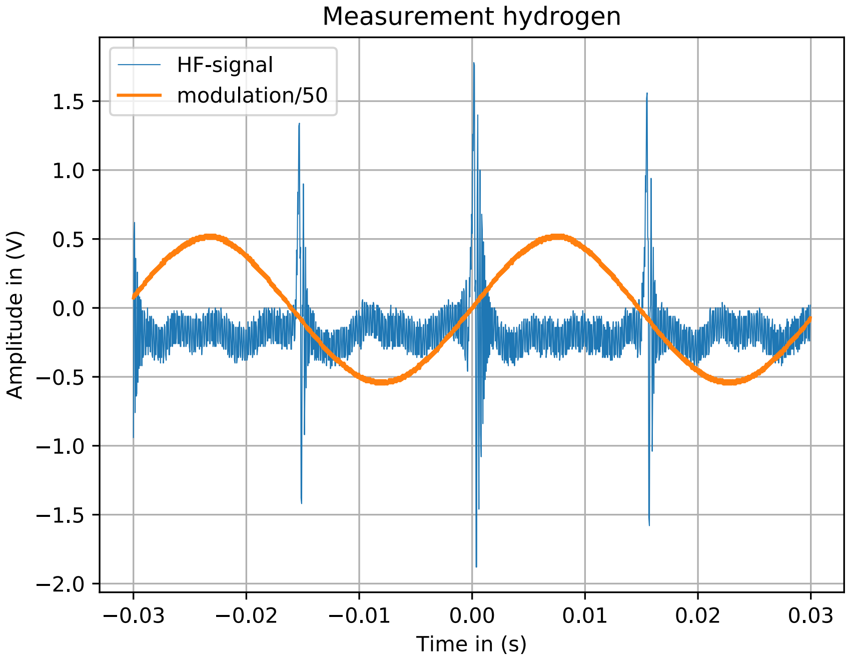

Figure 8: Data for resonance of a proton in hydrogen with the modulation signal that is shrunk by a factor of 50.

The frequency which we measured around is $\nu = (19.2970 \pm 0.0002)\,\text{MHz}$. The plots of the surrounding frequencies, which are needed in order to calculate the error on the frequency (see previous chapter), are overlaid in figure 9.

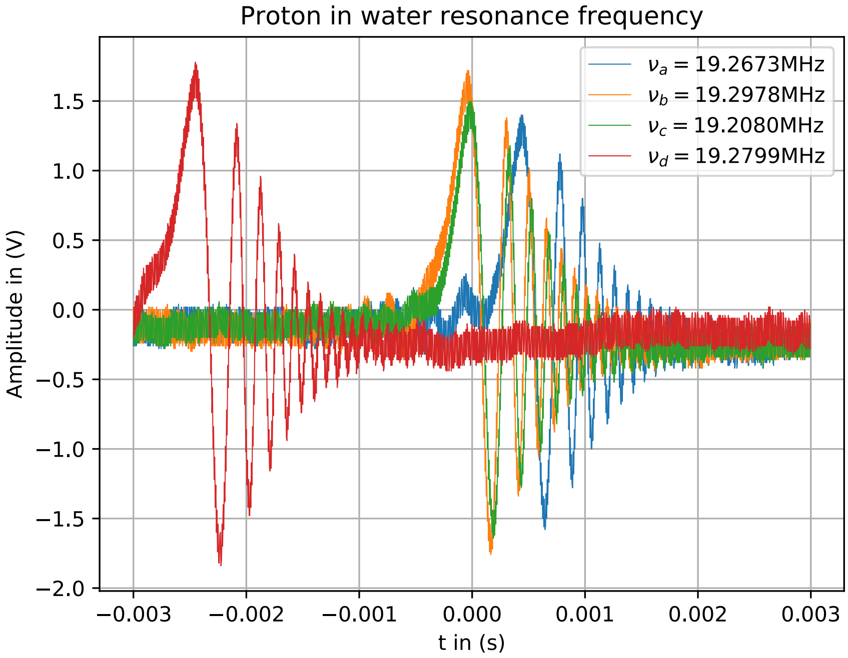

Figure 9: Method to determine the error of ν for hydrogen.

With the method described in the previous chapter (formula 4.1) we get as error $s_\nu = 0.07\,\text{MHz}$.

By adding it quadratic to the read-off error, our frequency then is

$$\boxed{\nu = (19.30 \pm 0.07)\,\mathrm{MHz}.}$$

In order to get the gyro magnetic factor we use formula 4.2 again which provides us with

$$\boxed{g_I = 5.616 \pm 0.012.}$$

Finally we want to get the gyro magnetic property of the proton in hydrogen. This we calculate with formula 4.3. The result is

$$\boxed{\gamma = (2.690 \pm 0.006) \cdot 10^8 \,\frac{\mathrm{rad}}{\mathrm{s\,T}}.}$$

4.4. Determination of the gyro magnetic property of a proton in glycol

In order to calculate the gyro magnetic property of a proton in glycol we chose a magnetic field of $B = (451.0 \pm 0.5)\,\mathrm{mT}$. The equal distance of the peaks in figure 10 (see also fig 31 for a screen shot of the oscillator) gave us a frequency of $\nu = (19.2970 \pm 0.0002)\,\mathrm{MHz}$.

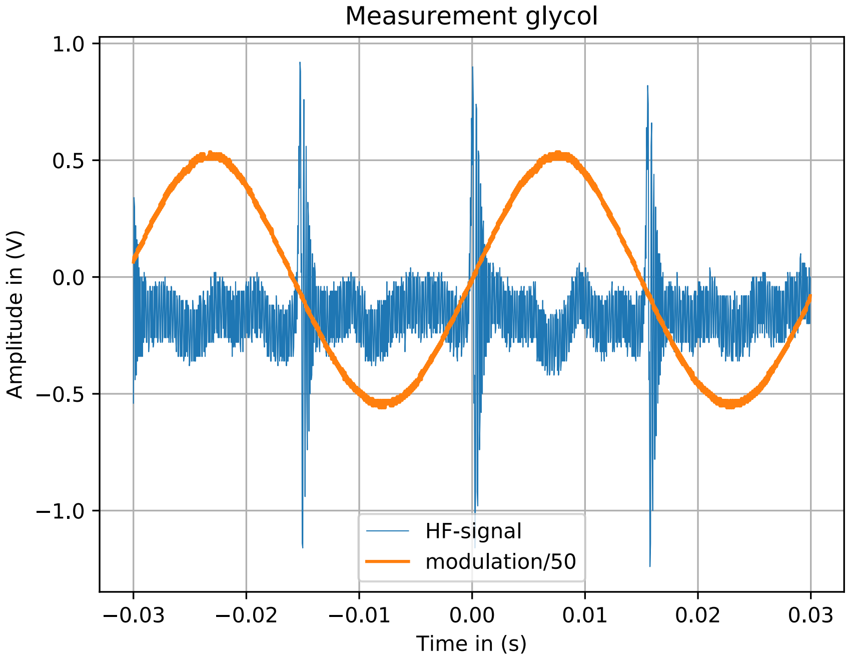

Figure 10: Data for resonance of a proton in glycol with the modulation signal that is shrunk by a factor of 50.

Around this frequency we measured the data, which is plotted in figure 11. We do this because we want to have equidistant peaks in figure 10 and need to know, whether the frequency we chose fulfils this condition. This method is chosen for all measurements in chapters 4.2 to 4.4, because the peaks are quiet broad and simply reading off of the error wouldn't be as precise.

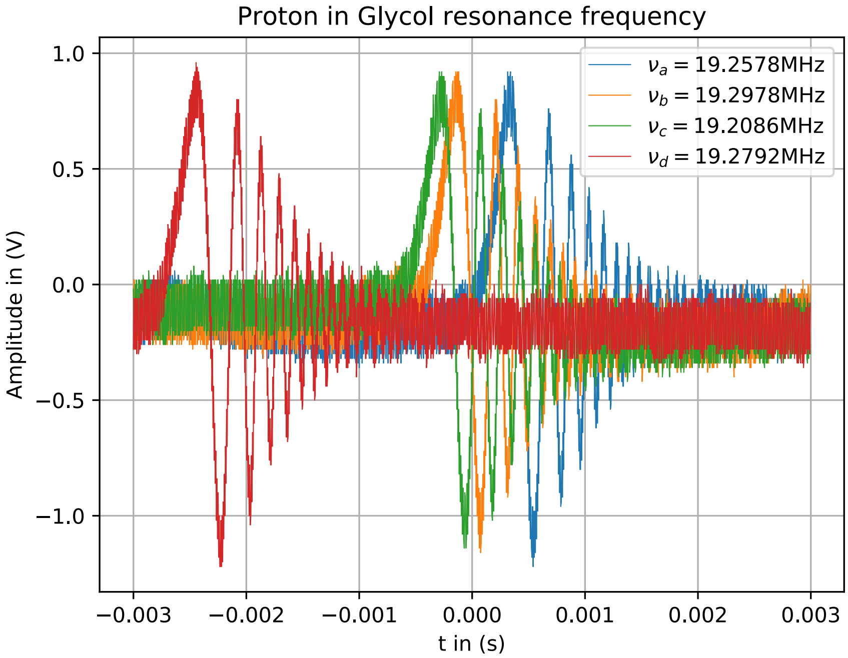

Figure 11: Method to determine the error of ν glycol.

This time formula 4.1 gave us an error of $s_{nu} = 0.08\,\mathrm{MHz}$ on the frequency. Following from this we get

$$\boxed{\nu = (19.30 \pm 0.08)\,\mathrm{MHz}.}$$

The gyro magnetic factor is, according to formula 4.2

$$\boxed{g_I = 5.616 \pm 0.012.}$$

The gyro magnetic property is calculated again with formula 4.3 and results in

$$\boxed{\gamma = (2.690 \pm 0.006) \cdot 10^8\,\frac{\mathrm{rad}}{\mathrm{s\,T}}.}$$

4.5. Fine measurement of the resonance frequency of a proton in hydrogen with the Lock-in-method

The parameters we chose on the synchron detector and for the saw tooth for this measurements are listed in table 2.

	synchron detector	saw tooth
time constant/period	0.3 s	10 s
amplitude	-	0.5 V
B-field	(452.0 ± 0.5) mT	

Table 2: Parameters, at which we measured with the lock-in method.

The method we used here is the so called Lock-in method. Instead of an absorption curve, its differential is used here. This means, that now the minimum of an absorption curve is a transition through zero. The modulation signal used this time is a saw tooth signal which has a sinus curve with a small amplitude superimposed. In order to get the transition through zero we measured eight times around the zero transition. Then we fitted linear approximations to the absorption signal and the saw-tooth signal. This was done with the `scipy.optimize.curve_fit` function from Python. From this we got a linear function

$$y = ax + b,$$

that allows to calculate the zero transitions by putting y to zero and solve the equation for x. The error on the x-axis gets calculated by varying the parameters of the fit function, meaning that we created separate lines using the errors for a and b:

$$\begin{aligned}
y_1 &= (a - s_a)x + (b) \\
y_2 &= (a - s_a)x + (b - s_b) \\
y_3 &= (a - s_a)x + (b + s_b) \\
y_4 &= (a + s_a)x + (b) \\
y_5 &= (a + s_a)x + (b - s_b) \\
y_6 &= (a + s_a)x + (b + s_b).
\end{aligned}$$

The lines with the biggest distance to the 'normal' line at $y = 0$ (i.e. on the x-axis) give us the error on x. As an example the plots for one measurement can be seen in figure 12 and 13. The others are shown in the appendix in figures 15 to 28.

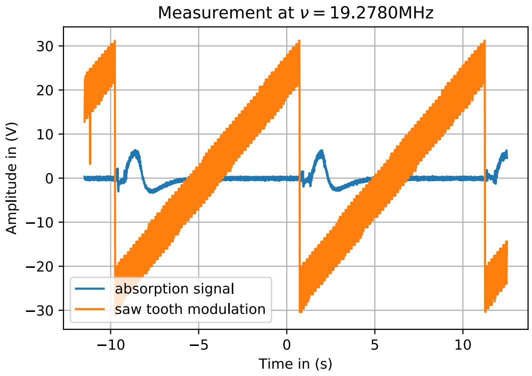

Figure 12: Measured Lock-in method data at $\nu = (19.2780 \pm 0.0002)\,\mathrm{MHz}$.

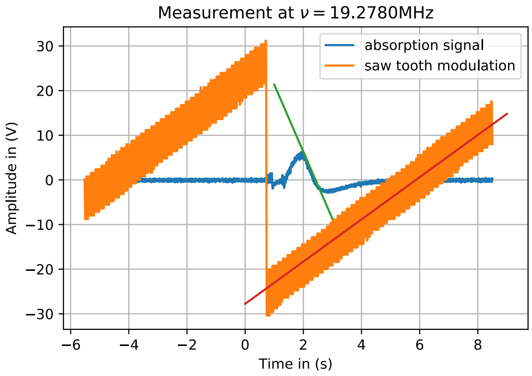

Figure 13: Enlargement from figure 12 with fits for the absorption and the saw tooth.

The frequencies at which we measured and their corresponding time differences between transitions through zero are listed in table 1. These time differences we calculated by subtracting the zero transition of the signal from that of the saw tooth. The error on the frequency is 0.05 MHz, because the frequency, while measuring, wasn't always constant, and that on the time difference 1.1 s. The error on the time difference was calculated by changing the parameters in the fit functions.

Frequency [MHz]	Time difference [s]
19.28	3.5
19.32	2.7
19.35	0.6
19.37	0.01
19.40	-2.4
19.46	-3.2
19.38	-0.7
19.30	2.7

Table 3: Time differences between zero intersection of the absorption and the modulating curve.

We have plotted this data in figure 14.

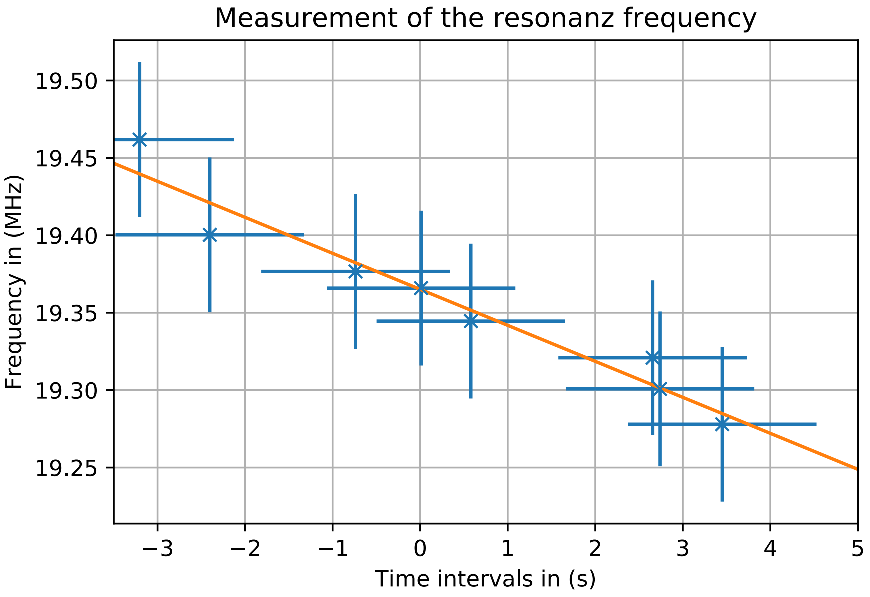

Figure 14: Determination of the resonance frequency.

The function, that describes this linear approximation is

$$(-0.0233 \pm 0.0002)x + (19.365 \pm 0.005).$$

This gives us the frequency for the time interval zero which corresponds with the y axis section. The error is calculated from the square root of the diagonal elements from the covariance matrix which we got by `scypy.optimize.curve_fit`. Putting this together we get for the frequency

$$\boxed{\nu = (19.365 \pm 0.005)\,\mathrm{MHz}.}$$

This now can be compared to the resonance frequency of hydrogen calculated in chapter 4.3, which is $\nu_H = (19.29 \pm 0.07)\,\mathrm{MHz}$. We can see, that the two values are in a 2σ range to one another. Looking at the relative errors, which are $\nu_{rel} = 0.026\,\%$ and $\nu_{H_{rel}} = 0.36\,\%$, we can say that the measurement methods are precise and the results meaningful.

5. Summary and discussion

The intention of the first experiment was to find out, whether there is a sufficient large enough, homogeneous magnetic field strength area created by our magnet or not. Our result can be seen in figure 5. We didn't reach the lower end of the magnetic field, because of some scotch tape on the tape measure, that made it very imprecise to measure underneath of 3 cm. But the area we measured was, from 0.7 cm on very homogeneous. This is also shown by the relative error of 0.2 %.

The execution of the next three parts were similar to each other. The goal of the first one was, to determine the core magnetic moment of a ^{19}F-core. In the second and third the gyro magnetic properties of a proton in hydrogen and glycol were to be determined.

	^{19}F	hydrogen	glycol
frequency ν [MHz]	19.24 ± 0.06	$\boxed{19.30 \pm 0.07}$	19.30 ± 0.08
gyromagnetic property γ [$10^8\,\mathrm{rads^{-1}T^{-1}}$]	2.520 ± 0.009	$\boxed{2.690 \pm 0.006}$	$\boxed{2.690 \pm 0.006}$
magnetic moment $\lvert\vec{\mu}\rvert$ [$10^{-8}\,\mathrm{eVT^{-1}}$]	$\boxed{2.286 \pm 0.009}$	-	-

Table 4: Experimental gathered data of parts 2 to 4.

$\gamma_{\text{prot}} = (2.675\,221\,900 \pm 0.000\,000\,018) \cdot 10^8\,\frac{\text{rad}}{\text{sT}}$ [2] is the theoretical value for the gyro magnetic property of a proton. This can be compared to the gyro magnetic properties of hydrogen and glycol. For both of them we have measured the same value. This makes sense, because in both measurements we had the absorption spectra of a single proton. The value from the literature is in their 3σ-range. For this there are some possible reasons. A problem at the measuring device was, that the modulation wheel for the frequency was not very precisely swivelling. Another problem was, that the signal sometimes jumped very fast in the direction of the y-axis. This made it complicated to get the absorption curve peaks on the transitions through the x-axis of the modulation curve. The process for getting the peaks equidistant, was also quite difficult and therefore this might also be a source of the difference to literature. Although two measurements are a bit few to very- or falsifier this, the fact, that both measurements lead to the same result leads us to the assumption, that there might be a systematic error. One reason for this might be, that the modulation graph wasn't put accurate enough onto the zero-line in the oscilloscope, which we used to see the zero transitions of the absorption amplitude. This error would be systematic, because we always kept this function in the same position. Another problem of the setup was, that the electric wires that connected the different devices were very sensible to movement and interference from other electronic devices. An even bigger difference between the one we measured and the literature value was for the magnetic moment of ^{19}F in Teflon. The theoretical value here is $\mu_{lit} = 2.628\,87 \cdot 10^{-8}\,\frac{\text{eV}}{\text{T}}$ [5]. This is in the range of 39σ. Here the error sources are the same as before. But because of this big difference, we also tried, whether we had chosen the errors too small. For this we measured the time difference between two peaks in the plots. We guessed an error of 0.001 s on the time difference we read off. This gave us then a magnetic moment of $|\vec{\mu}| = (2.29 \pm 0.12)\,\frac{\text{eV}}{\text{T}}$. This is 3σ away from the theoretical value. With a relative error of 5.2 % we can conclude that the estimation of the error for the distance would have been a valid option for the error calculations and would have given us reasonable results.

The last part was about using the lock-in method to measure the resonance frequency of hydrogen. The result we get here is $\nu_{Lock} = (19.365 \pm 0.005)\,\text{MHz}$. This we compare to the frequency measured in the third part (reminder, this value was $\nu = (19.30 \pm 0.07)\,\text{MHz}$). As we can see the result measured with the Lock-in method is in a 2σ interval of the one measured previously.

This fits very nicely, but by comparing the relative errors for the lock-in it is 0.026 % and for the other one 0.36 %, we can see, that the results we get from the lock-in method are more precise. This is also the result we would have expected, because the transition of the absorption signal through zero amplitude is easier to detect than the maxima in the measurement without lock-in.

So what we did in this experiment was to look, whether the magnetic field in the set up was homogeneous and calculated the core magnetic moment of ^{19}F and the gyro magnetic property of a proton in hydrogen and glycol. Finally we tested another method for measuring the resonance frequency of protons in hydrogen, the lock-in method, and compared it to the value we measured before.

A. List of Figures

1. Differentiated absorption signal [1]. 7
2. Setup for the measurement of the magnetic field [1]. 8
3. Setup for the measurements in exercise 2, 3 and 4 [1]. 9
4. Setup for the measurement in exercise 5 [1]. 9
5. The value of the measured magnetic field plotted against the depth of the hall probe. 11
6. Data for ^{19}F with the modulation signal that is shrunk by a factor of 50. 12
7. Method to determine the error of ν for ^{19}F. 13
8. Data for resonance of a proton in hydrogen with the modulation signal that is shrunk by a factor of 50. 15
9. Method to determine the error of ν for hydrogen. 15
10. Data for resonance of a proton in glycol with the modulation signal that is shrunk by a factor of 50. 16
11. Method to determine the error of ν glycol. 17
12. Measured Lock-in method data at $\nu = (19.2780 \pm 0.0002)\,\mathrm{MHz}$. 18
13. Enlargement from figure 12 with fits for the absorption and the saw tooth. 18
14. Determination of the resonance frequency. 19
15. Measured Lock-in method data at $\nu = (19.3008 \pm 0.0002)\,\mathrm{MHz}$. 24
16. Enlargement from figure 15 with fits for the absorption and the saw tooth. 24
17. Measured Lock-in method data at $\nu = (19.3209 \pm 0.0002)\,\mathrm{MHz}$. 24
18. Enlargement from figure 17 with fits for the absorption and the saw tooth. 24
19. Measured Lock-in method data at $\nu = (19.3446 \pm 0.0002)\,\mathrm{MHz}$. 24
20. Enlargement from figure 19 with fits for the absorption and the saw tooth. 24
21. Measured Lock-in method data at $\nu = (19.3659 \pm 0.0002)\,\mathrm{MHz}$. 25
22. Enlargement from figure 21 with fits for the absorption and the saw tooth. 25
23. Measured Lock-in method data at $\nu = (19.3767 \pm 0.0002)\,\mathrm{MHz}$. 25
24. Enlargement from figure 23 with fits for the absorption and the saw tooth. 25
25. Measured Lock-in method data at $\nu = (19.4003 \pm 0.0002)\,\mathrm{MHz}$. 25
26. Enlargement from figure 25 with fits for the absorption and the saw tooth. 25
27. Measured Lock-in method data at $\nu = (19.4618 \pm 0.0002)\,\mathrm{MHz}$. 26
28. Enlargement from figure 27 with fits for the absorption and the saw tooth. 26
29. Screenshot of oscillator for ^{19}F. 26
30. Screenshot of oscillator for hydrogen. 27
31. Screenshot of oscillator for glycol. 27

B. List of Tables

1. Data of the measurement of the magnetic field with $s_B = 0.5\,\mathrm{mT}$ and $s_d = 0.1\,\mathrm{cm}$. 11
2. Parameters, at which we measured with the lock-in method. 17
3. Time differences between zero intersection of the absorption and the modulating curve. 19
4. Experimental gathered data of parts 2 to 4. 20

C. References

[1] A. Ortner et al., *Versuchsanleitung Fortgeschrittenen Praktikum Kernspinresonanz*, Physikalisches Institut, Fakultät für Mathematik und Physik, Albert-Ludwigs-Universität Freiburg

[2] Drs. Taylor and Mohr, *The NIST Reference on Constants, Units and Uncertainty*, in: Website of the National Institute of Standarts and Technology, 2014, `https://physics.nist.gov/cuu/index.html`, looked for at September 6, 2018

[3] D. Freude *4 Die magnetische Kernresonanz* , in: Spektroskopie, 2006, `http://home.uni-leipzig.de/energy/pdf/freusd4.pdf`, looked for at September 6, 2018

[4] Ann. Magn. Reson., Vol. 1, No 1, 43-64, 2002 *NMR NOMENCLATURE: NUCLEAR SPIN PROPERTIES AND CONVENTIONS FOR CHEMICAL SHIFTS (IUPAC Recommendations 2001)*

[5] ©1996 - 2018 Internetchemie ChemLin, `https://www.internetchemie.info/chemie-lexikon/daten/n/nmraktivekerne.php`, looked for at September 6, 2018

[6] T. D. W. Claridge, *High Resolution NMR Techniques in Organic Chemistry*, Chapter 2; E. Breitmaier, W. Voelter, Carbon 13 NMR Spectroscopy,3rd Ed., 3.3.2. `https://www.colby.edu/chemistry/PChem/lab/Spinlattice.pdf`

D. Appendix

D.1. Additional Plots

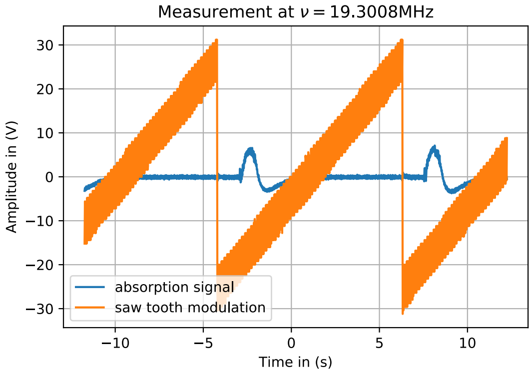

Figure 15: Measured Lock-in method data at $\nu = (19.3008 \pm 0.0002)$ MHz.

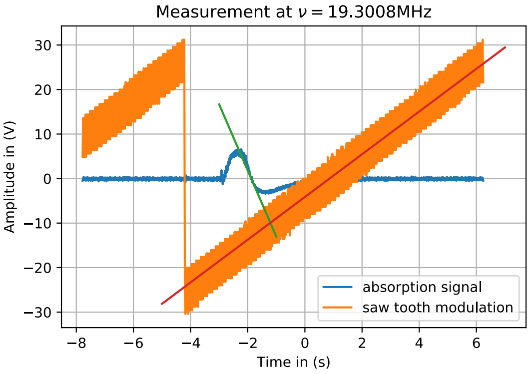

Figure 16: Enlargement from figure 15 with fits for the absorption and the saw tooth.

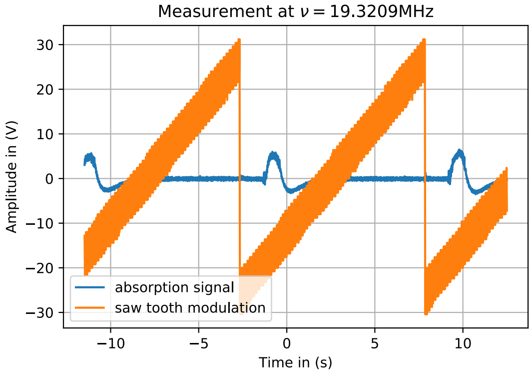

Figure 17: Measured Lock-in method data at $\nu = (19.3209 \pm 0.0002)$ MHz.

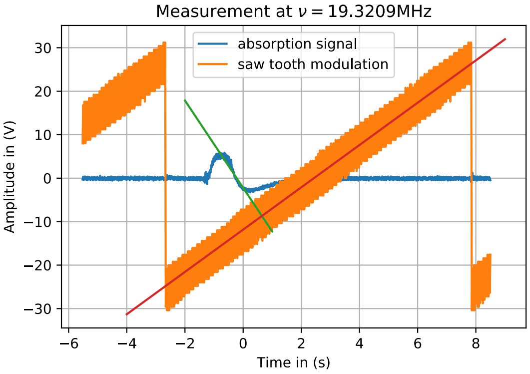

Figure 18: Enlargement from figure 17 with fits for the absorption and the saw tooth.

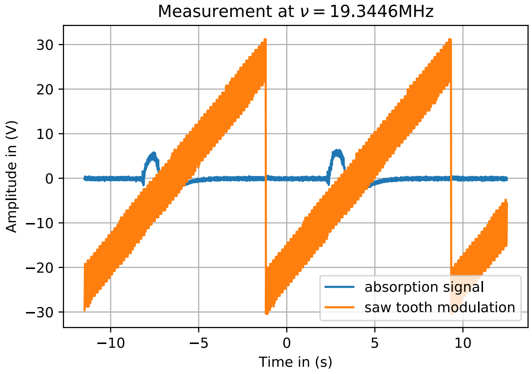

Figure 19: Measured Lock-in method data at $\nu = (19.3446 \pm 0.0002)$ MHz.

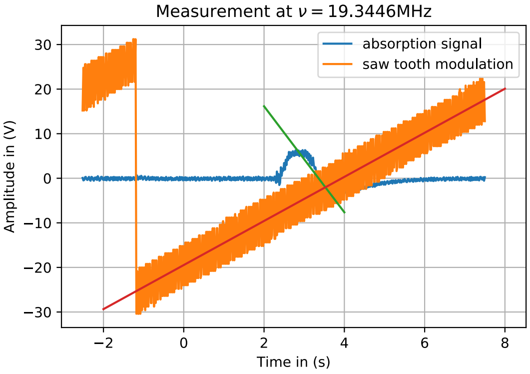

Figure 20: Enlargement from figure 19 with fits for the absorption and the saw tooth.

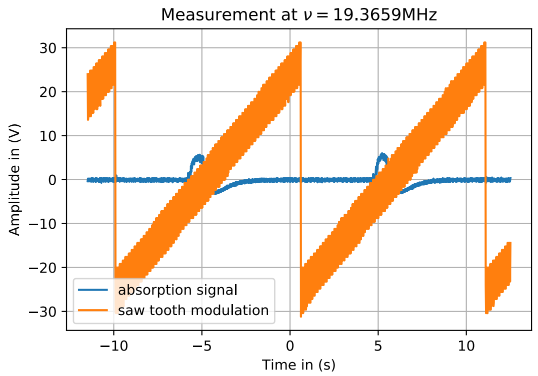

Figure 21: Measured Lock-in method data at $\nu = (19.3659 \pm 0.0002)$ MHz.

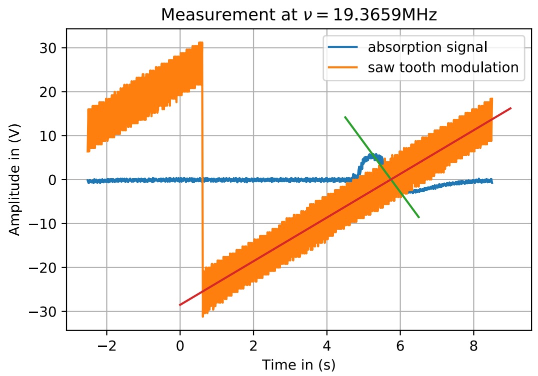

Figure 22: Enlargement from figure 21 with fits for the absorption and the saw tooth.

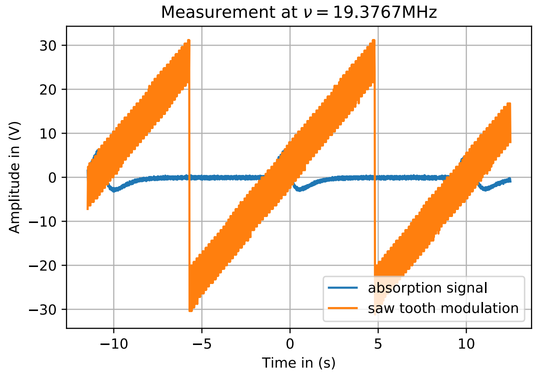

Figure 23: Measured Lock-in method data at $\nu = (19.3767 \pm 0.0002)$ MHz.

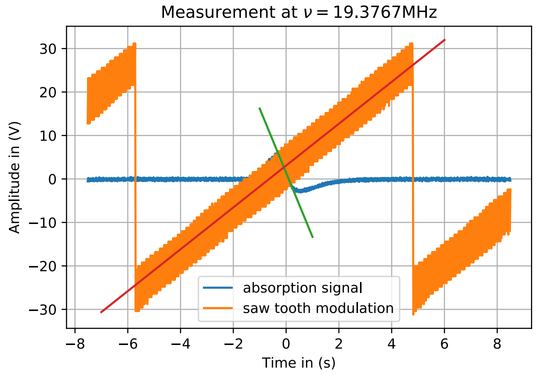

Figure 24: Enlargement from figure 23 with fits for the absorption and the saw tooth.

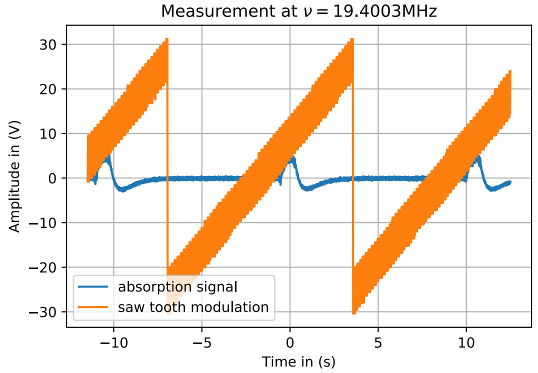

Figure 25: Measured Lock-in method data at $\nu = (19.4003 \pm 0.0002)$ MHz.

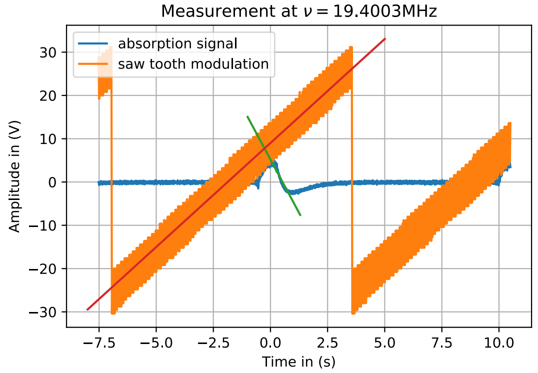

Figure 26: Enlargement from figure 25 with fits for the absorption and the saw tooth.

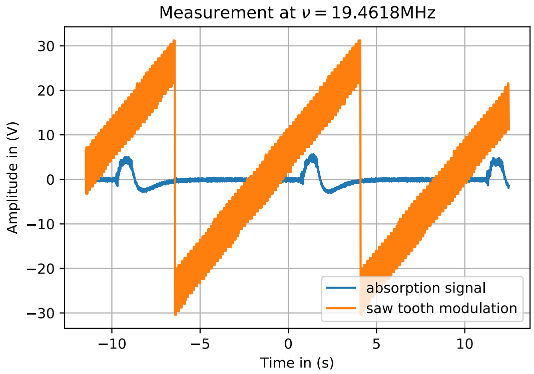

Figure 27: Measured Lock-in method data at $\nu = (19.4618 \pm 0.0002)\,\mathrm{MHz}$.

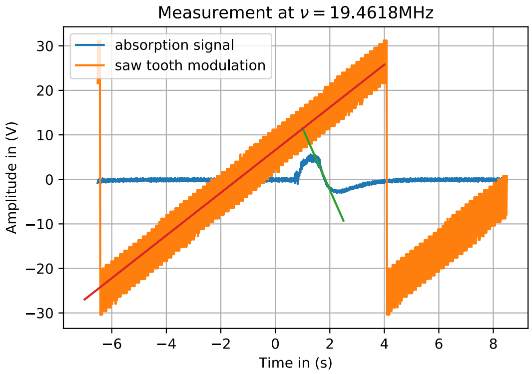

Figure 28: Enlargement from figure 27 with fits for the absorption and the saw tooth.

D.2. Oscilloscope screenshots

Period=30.80ms

Freq=32.5 Hz

Figure 29: Screenshot of oscillator for ^{19}F.

Period=30.80ms
Freq=32.5 Hz

Figure 30: Screenshot of oscillator for hydrogen.

Period=30.80ms
Freq=32.5 Hz

Figure 31: Screenshot of oscillator for glycol.

D.3. Original data

31.8.18

Kernspinresonanz

Vermessung des Magnetfelds mit Hallsonde

~~Höhe [cm]~~	~~B-Feld [mT]~~
~~3,3~~	~~464~~
~~3,0~~	~~465~~
~~2,7~~	~~465~~
~~2,4~~	~~465~~
~~2,2~~	~~465~~
~~1,8~~	~~464~~
~~1,4~~	~~463~~
~~1,0~~	~~464~~
~~0,8~~	~~463~~
~~0,6~~	~~462~~
~~0,2~~	~~460~~

Hallsonde schräg

$s_y = 0{,}1\,\text{cm}$
$s_B = 1\,\text{mT}$

~~$U = 9\,\text{V}$~~
~~$I = 3{,}73\,\text{A}$~~

19F-Kern Kernmagnetisches Moment

~~18,80 ms~~

~~1) 19,1781 MHz~~
~~2) 19,1847 MHz~~
~~3) 19,1733 MHz~~

falsch gemessen

~~19,0263 MHz~~

2. Kernmagnetisches Moment 19F

Fehler:
$s_\nu = 0,0002$ MHz

B-Feld: 473 mT

19,0075 MHz

$\nu_a = 18,9089$ MHz
$\nu_b = 18,9977$ MHz
$\nu_c = 18,9080$ MHz
$\nu_d = 18,9982$ MHz

3. gyromagn. Verhältnis des Protons in Wasserstoff

Messen alles

B-Feld: 453 mT

19,2075 MHz

$\nu_a = 19,2575$ MHz
$\nu_b = 19,3902$ MHz
$\nu_c = 19,3016$ MHz
$\nu_d = 19,3228$ MHz

4. gyromagnetisches Verhältn. des Protons in Glykol

B-Feld: 454 mT

19,3528 MHz ← Daten

$\nu_a = 19,3724$ MHz
$\nu_b = 19,3538$ MHz
$\nu_c = 19,3040$ MHz
$\nu_d = 19,3356$ MHz

5. Feinvermessung bei Wasserstoff mit Lock-in-Verfahren

B-Feld: 452 mT

Zeitkonst Synchrondet.: 0,3
Sägezahn: 10

Ampl. Sägezahn: 0,5

1. 19,2780 MHz
2. 19,3209 MHz
3. 19,3446 MHz
4. 19,3659 MHz
5. 19,4003 MHz
6. 19,4618 MHz
~~7. 19,5000 MHz~~ zu hoch
7. 19,3767 MHz
8. 19,3008 MHz

Vermessung des Magnetfelds mit Hall-Sonde

s_B = ~~1 mT~~ 1 mT
s_y = 0,1 cm

U = 9,0 V
A = 4,08 A

Höhe [cm]	B-Feld [mT]
0	474
0,4	488
0,7	489
1,0	489
1,3	489
1,6	489
2,0	~~490~~ 489
2,3	489
2,7	489
3,0	489
0,2	485
0,1	479

2. Kernmagnetisches Moment ^{19}F

s_ν = 0,0002 MHz

B-Feld : 473 mT

ν = ~~18,9072 MHz~~
18,9966 MHz
ν_a = 18,9467 MHz
ν_b = 18,9969 MHz
ν_c = 18,9071 MHz
ν_d = ~~18,8977 MHz~~
18,9079 MHz

0,0006 MHz
oder NewFolder 2

3. Proton in Wasserstoff

B-Feld : ~~453 mT~~ 451 mT

ν = 19,2970 MHz

NewFolder 3

ν_a = 19,2673 MHz
ν_b = 19,2978 MHz
ν_c = 19,2090 MHz
ν_d = 19,2799 MHz

4. Proton in Glycol

B-Feld: 451 mT

$\nu = 19,2970$ MHz

$\nu_a = 19,2578$ MHz
$\nu_b = 19,2978$ MHz
$\nu_c = 19,2086$ MHz
$\nu_d = 19,2792$ MHz

2. Kernmagnetisches Moment ^{19}F

B-Feld: ~~801 mT~~ 480 mT

$\nu = 19,2396$ MHz

$\nu_a = 19,2884$ MHz
$\nu_b = 19,2985$ MHz
$\nu_c = 19,2030$ MHz
$\nu_d = 19,3807$ MHz